Fish passage through hydropower turbines: Simulating blade strike using the discrete element method

M C Richmond*, P Romero-Gomez
Pacific Northwest National Laboratory, Earth Systems Science Division, Hydrology Group, Richland, WA. 99352

E-mail: marshall.richmond@pnnl.gov

Abstract. Among the hazardous hydraulic conditions affecting anadromous and resident fish during their passage though hydro-turbines two common physical processes can lead to injury and mortality: collisions/blade-strike and rapid decompression. Several methods are currently available to evaluate these stressors in installed turbines, e.g. using live fish or autonomous sensor devices, and in reduced-scale physical models, e.g. registering collisions from plastic beads. However, *a priori* estimates with computational modeling approaches applied early in the process of turbine design can facilitate the development of fish-friendly turbines. In the present study, we evaluated the frequency of blade strike and rapid pressure change by modeling potential fish trajectories with the Discrete Element Method (DEM) applied to fish-like composite particles. In the DEM approach, particles are subjected to realistic hydraulic conditions simulated with computational fluid dynamics (CFD), and particle-structure interactions—representing fish collisions with turbine components such as blades—are explicitly recorded and accounted for in the calculation of particle trajectories. We conducted transient CFD simulations by setting the runner in motion and allowing for unsteady turbulence using detached eddy simulation (DES), as compared to the conventional practice of simulating the system in steady state (which was also done here for comparison). While both schemes yielded comparable bulk hydraulic performance values, transient conditions exhibited an improvement in describing flow temporal and spatial variability. We released streamtraces (in the steady flow solution) and DEM particles (transient solution) at the same locations where sensor fish (SF) were released in previous field studies of the advanced turbine unit. The streamtrace-based results showed a better agreement with SF data than the DEM-based nadir pressures did because the former accounted for the turbulent dispersion at the intake using an empirical method, but the unsteady simulation underestimated turbulence in the intake. However, the DEM-based strike frequency is more representative of blade-strike probability as compared to the steady solution, mainly because DEM particles accounted for the full fish length and width, thus resolving (instead of modeling) the collision event. Although further development and testing is needed, the DEM method shows promise as another tool in the engineering design process to develop turbines that can achieve fish-friendly hydraulic conditions.

1. Introduction

The environmental impacts of hydroelectric dams have long been recognized, studied, and, guided by research, mitigated by the hydropower industry in many cases. Various strategies to reduce the negative impacts of dams on aquatic biota, and on fish in particular, are commonly

analyzed and implemented at many hydropower installations in the U.S. and the developed world. For instance, spillways, bypass systems, and fish transportation are alternatives to turbine passage that can be safer, in some cases, for fish passage past dams during downstream migration [1]. However, some fraction of the fish population inevitably travels through the turbines, potentially encountering hazardous passage conditions [2, 3]. For that reason, field tests of fish survival through operating turbine units are being conducted in river systems with hydropower production, such as the Columbia river extending over the U.S. Pacific Northwest and Canada (see [4] for an example). Field evaluations are desirable but must be conducted after the turbine is designed, installed, and placed in operation. Thus, numerical model-based estimates of the hazardous conditions, based on laboratory experiments of fish response to hydraulic stressors found in turbine flows, would be advantageous considering the effort involved in preparing and conducting field tests. The present study uses advanced turbulence and particle modeling schemes to evaluate the blade strike frequency and nadir pressure environment that juvenile fish may potentially encounter in a Kaplan turbine at a typical operating point.

The main objective of this work was to determine the quantitative impact that two particle modeling schemes, Lagrangian spheres and Discrete Element Method (DEM), have on estimating the biological performance of a full-scale hydropower turbine. Figure 1 shows the steps followed to achieve the stated objective. To begin with, we conducted CFD flow simulations with two turbulence modeling approaches: Reynolds-averaged Navier-Stokes (RANS) and detached eddy simulation (DES). Next, we compared the simulated outcomes to plant estimates of power output and net head from the turbine. The predicted hydraulic conditions were then used to determine potential pathways of a fish sample during passage (see examples in figure 2). Three modeling techniques were used to the latter purpose: streamtraces through the RANS solution, and both Lagrangian and DEM particle tracking through the DES results. These trajectories provided the input information to quantify the magnitudes of two injury mechanisms affecting fish during passage: blade-strike and rapid decompression. The former risk was quantified as the frequency of strike events recorded from a passed fish sample, whereas the latter was evaluated as the lowest (nadir) pressure along each modeled trajectory. In previous studies of biological performance, the origin of the fish particle —streamtrace or particle — has been a key variable that affects the outcomes of biological performance assessments [5]. Therefore, we released particles from the same location of injection pipe outlets from which live and sensor fish were previously released in field tests at the same dam, for the same turbine, and the same flow conditions as those used in this study. In this way, we were able to directly compare the simulated stressor magnitudes against sensor fish data previously reported and published [4, 6].

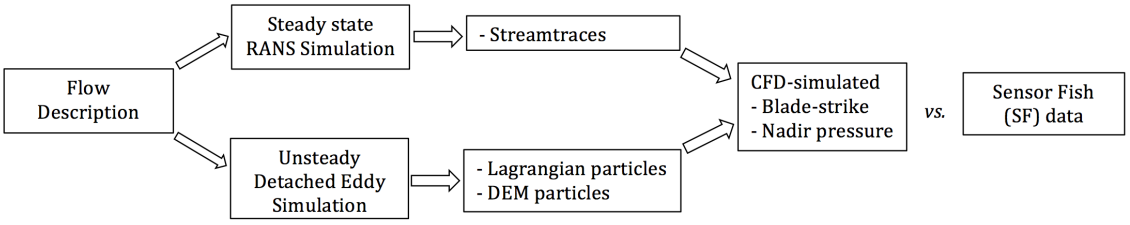

Figure 1. Workflow to determine the influence of turbulence modeling on the hydraulic and biological performance of a hydropower turbine.

2. Flow Modeling Approaches

2.1. Field conditions and Turbine Unit Description

The Wanapum Dam, owned and operated by Public Utility District No.2 of Grant County, is located on the Columbia River in central Washington State, at river km 668 where the annual average discharge is 3398 m^3/s. Wanapum dam has been in operation since 1963, and the original 10 Kaplan turbine units began to be replaced in the mid-2000s to improve both the hydraulic and environmental performance. In this study, we studied a single unit of the new advanced turbine type designed and manufactured by Voith Hydro, which consists of a six-blade turbine with spherically-shaped hub and discharge ring to minimize gaps that are known to be hazardous to fish passage and detrimental to power generation efficiency. A description of the advanced turbine in the context of recent trends in environment-friendly hydropower turbines is provided in a recent review paper [7].

The simulated system included the turbine runner, as well as the intake and draft tube (see figure 2). The intake features a distributor with 32 wicket gates and 16 stay vanes to guide the incoming flow into the turbine. The design of the draft tube was also enhanced during the turbine replacement to reduce flow recirculation and other energy losses that directly impact the unit hydraulic efficiency.

A discharge (Q) of 472.13 m^3/s and gross head of 23.45 m were selected as the operating point for the simulations. At these conditions, the field estimate for net head was 22.95 m, for shaft output power was 99.14 MW, and for unit efficiency was 93.3%. The Wanapum turbines have been field tested using sensor fish devices [8, 9]. In addition, balloon tagged live fish were used to estimate the direct survival associated with turbine passage [10]. Detailed information regarding the site, the turbine unit,and the hydraulic test conditions has been previously reported by [4]. We simulated one discharge scenario included in these field studies, denoted as the "17 kcfs" nominal discharge case. The CFD models were run using the gross head differential between the forebay and tailrace water elevations as the boundary condition driving the flow.

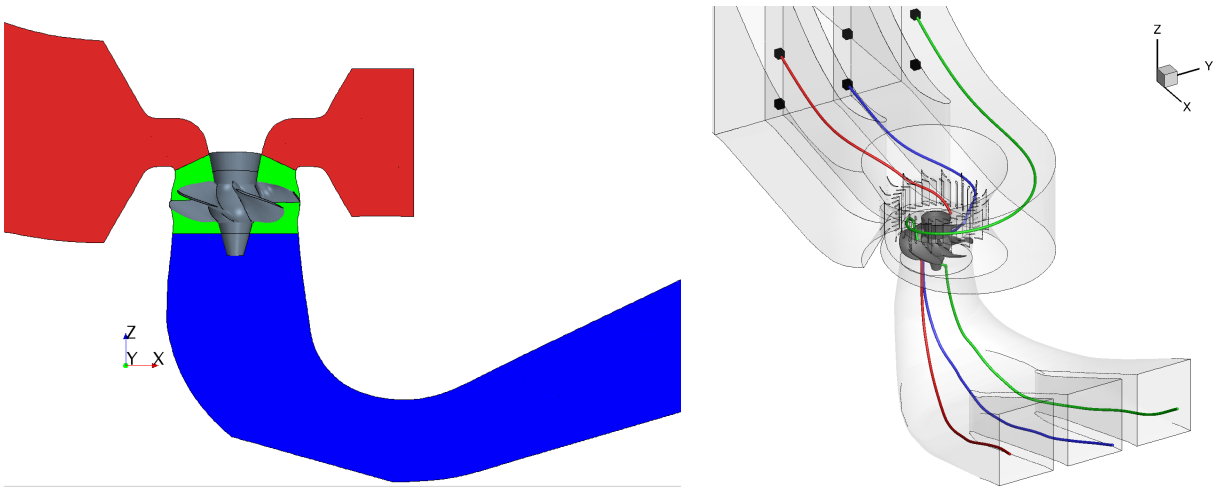

Figure 2. The model included the six-bladed Kaplan turbine, as well as the intake and draft tube (left), and streamtraces starting from the field test release pipes located in the intake showing the six injection locations (right).

2.2. CFD: Reynolds-Averaged Navier-Stokes

Steady-state turbine flow conditions were simulated in a full-scale model of the turbine system. The commercial code STAR-CCM+ v8 [11] was used to generate an unstructured mesh with

34.3M primarily hexahedral cells to discretize a domain divided into three regions: intake, runner, and draft tube/exit (figures 2). The cell allocation varied per region: 13.6M, 14.0M, 6.7M cells, respectively. The cell density varied spatially within each region, with more cells located near the walls to capture large flow gradients in the boundary layers. The averaged y^+ value for the first layer of cells off the wall was $\sim$20 on the blade surface. The intake region included the stay vanes and wicket gates, as well as a porous baffle representing the pressure drop from the trash racks. A moving frame of reference was applied at the runner region to account for the runner rotation, with a rate of 8.98 rad/s (85.7 RPM). The transition between this moving reference frame and the stationary frame of the draft tube was represented by an indirect interface scheme in which the flow quantities were circumferentially averaged as commonly practiced in steady-state turbo-machinery applications. The flow rate resulted from setting up a pressure differential between the inlet and outlet boundaries equal to the gross head from the field data (23.45 m). The segregated flow solver used a 2^{nd}-order discretization scheme for the convection term, and the κ-ω SST turbulence model was used to compute the Reynolds stresses from the eddy viscosity. The pressure drop through the interface representing the trash racks followed the conventional two-term formulation with a porous internal resistance of 0.051 but no viscous resistance, and a porosity of 82.5% derived from the ratio of the "open area" projected on the x-direction to the total trash rack area (height $\times$ width). A mesh sensitivity test of the model was conducted with sizes of 1.3M, 2.5M, 6.9M, 28.0M and 34.3 cells. No significant difference in bulk hydraulic performance was observed from the RANS simulations with the two densest grids, and the latter (34.3M) was selected because of the need for spatial refinement in corresponding transient DES runs.

2.3. CFD: Detached Eddy Simulation

Transient turbine hydraulics were simulated using the DES version of the κ-ω SST turbulence model in STAR-CCM+. Although the geometry, boundary conditions, flow solver settings, and other features remained the same as for the RANS simulation, the DES run had additional requirements over the RANS counterpart. For instance, modeling the potential interactions between real-size fish DEM particles and an actual operating turbine required the runner region be set as a rigid body in rotating motion using sliding mesh interfaces between the stationary intake and draft tube zones. This in turn required the solution timestep be constrained by the Courant number in the form $\frac{V_{tip} \times \Delta t}{\Delta x} \approx 1$, which resulted in $\Delta t = 0.005$ s for the blade tip velocity (V_{tip}) and the averaged cell size (Δx) interfacing between the moving runner and stationary regions. The flow simulation was warmed up over a period of 60 seconds until a statistical average was reached, and then particle tracking was conducted over 60 additional seconds of simulation time.

3. Fish Passage Modeling Approaches

CFD-simulated flow conditions aided in the evaluation of fish exposure to two stressors that are known to cause mortal injury during passage: blade-strike occurrence and rapid decompression. Flow simulations provided the input data to calculate the potential fish pathways during passage through the hydropower turbine. Using these pathways, two quantities were determined: (a) the interactions between the fish-like particles and the rotating blades were recorded, and (b) the lowest pressure along each calculated trajectory was sampled. This scheme has previously been used with streamtraces generated for steady-state, RANS flow solutions [5, 12]. Figure 2 shows an example of three streamtraces through the unit. With a transient, DES-based flow solution, we aimed at achieving two enhancements: first, the strike event with particles is explicitly resolved instead of being modeled with a probabilistic formulation, and second, the unsteady results provide a better description of the transient turbulent conditions, compared to a steady RANS solution.

Juvenile salmonid fish are subjected to potential mortal injury as they pass through turbines during their downstream migration. We assumed a generic fish length (L) of 10 cm and a mass ($\bar{m}_p$) of 14 g as representative of juvenile salmonids [13]. In representing a fish body, the modeled particle can vary in complexity and shape, which in turn have an influence on the computational expense to determine the fish pathways (see figure 3). In this study, we modeled the fish body (fig. 3a) using the following methods (listed in decreasing modeling complexity): a composite particle for discrete element modeling or DEM (fig. 3b), a spherical Lagrangian particle (fig. 3c), and an advected massless particle (fig. 3d). The stressor statistics (blade strike and nadir pressure) are very sensitive to the release location of these model particles. We released the particles from seeds located at six pipe exits from which sensor and live fish were also released in the field tests [4, 6]. Three release points are located at each bay center 3.04 m below the intake ceiling ("10-ft pipes"), while three more are located 9.14 m ("30-ft pipes") below the turbine ceiling (figure 2). In this work, we grouped the modeling results per "pipe-elevation" to establish direct comparisons to the sensor fish data provided from previous work [4, 6]. These past studies include details of the field conditions as well as descriptions of the sensor fish data used in this work.

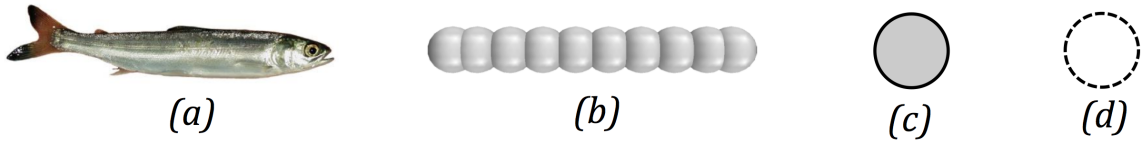

Figure 3. The representation of 10-cm juvenile fish (a) depended on the modeling scheme for fish particles: (b) a composite particle was used in DEM, (c) a material particle was used in the Lagrangian scheme, and (d) a massless particle was advected to determine streamtrace-based pathways

3.1. Streamtraces

The simplest way to numerically represent fish paths is as a massless particle (fig. 3d) seeded at the release points and advected through the domain, assuming that the particle velocity ($\bar{u}_p$) is equal to the flow velocity ($\bar{u}$). This pathway represents a case in which fish are passively carried along with the flow, with no drag, no lift or any other body or surface force acting on the fish. In this strategy, the data analysis package Tecplot360^{TM} (Tecplot, Inc., Bellevue, Washington) was used to calculate the streamtraces, and to conduct the sampling of nadir pressures and the modeling of strike probability. A major assumption from this method is that only the leading edge of the blade contributes to the strike probability. Previous studies included the details of the modeling procedure and underlying assumptions, as well as the seeding strategy in the case of a few discrete release locations such as in this application. A sample of seeds surrounding the release pipe is run to conduct the statistical analysis. More information can be found in previously published documents [5, 12]. Streamtraces were computed using the steady RANS flow solution.

3.2. Lagrangian Particles

Fish represented as spherical Lagrangian particles with mass (fig. 3c) add additional physical realism compared to streamtraces albeit at increased computation effort. Lagrangian particles are not simply passively advected through the flow but instead, the particle velocity ($\bar{u}_p$) is determined by solving an ordinary differential equation (equation 1) that includes the fluid forces acting on the particle such as drag ($\bar{F}_d$), pressure gradients ($\bar{F}_p$), virtual mass effects

($\bar{F}_{vm}$), and gravity ($\bar{F}_g$) when fish are made non-neutrally buoyant. The detailed formulation for each force can be found in the STAR-CCM+ code documentation [11]. A neutrally buoyant sphere must be 3 cm in diameter to obtain the target fish mass ($\bar{m}_p = 14$ g).

Spheres were injected from the release points over a period of 20 seconds, at a rate of 8 particles-per-second per injection point, for a total of 960 spheres (480 per "pipe elevation"). The absolute pressure of the surrounding fluid is recorded along the particle trajectory. A boundary sampling scheme recorded the interactions between the spheres and blade surfaces. These interactions represented strike events. The boundary sampling included other quantities associated with the strike event such as its location, impact velocity, residence time, etc. This information is relevant to conduct future studies of mortality associated with the strike conditions. However, the latter analysis is not included in the present work. From the Lagrangian particle solver, we determined the strike frequency (F_{lag}) as the ratio of number of striking particles to the number of released particles. A particle with multiple strike events counts as a single striking particle.

$$m_p \frac{d\bar{u}_p}{dt} = \bar{F}_d + \bar{F}_p + \bar{F}_{vm} + \bar{F}_g \tag{1}$$

3.3. Composite Discrete Element Method Particles

The next level of fish representation corresponded to a discrete element particle that spans the target fish length (L) by compositing a number of spherical sub-particles (fig. 3b). The tracking algorithm for composite particles is conceptually the same as for spherical particles: a momentum balance equation is solved, the fluid forces determine the particle motion, and the interactions between particles and blade surfaces can be recorded to detect strike events. However, the DEM particles add a number of advantages over spherical particles: the fish length —known to be important in fish passage survival— is fully represented, interactions between the blades and any contact point of the DEM particle surface —as opposed to only the centroid-blade interactions as with spheres— are detected, and the angular momentum balance equation solves for the particle orientation. The latter 6 degree of freedom (6DOF) feature is particularly beneficial because fish orientation has been observed to be critical in estimating fish survival during blade strike [4, 14–16]. The formulation of each force term in equation 1 is modified to account for the composed shape of the DEM particle by including the concept of sphericity. Details can be found in the code documentation [11].

The DEM particle injection strategy is the same as for spherical particles, and the strike frequency (F_{dem}) is also the ratio of the number of striking DEM particles to the number of released DEM particles. A particle with multiple strike events counts as a single striking particle.

4. Results and Discussion

4.1. Simulated flow conditions: RANS vs. DES

Figure 4 shows a qualitative comparison of the flow conditions arising from both turbulence modeling schemes. Both figures show the iso-surfaces of Q-criterion at 10 s^{-2} in the draft tube, as calculated from the steady RANS and an instantaneous time slice from the transient DES. The Q-criterion [17] is a numerical quantity used to visualize the vortex rope developing under the hub as the fluid begins to diffuse into the draft tube. Both the RANS and DES solutions exhibit the vortex rope, but the qualitative appearance in RANS suggests that the instability remains contained within a smaller volume, and that the flow mixing takes place more rapidly, as compared to the DES solution.

Although not shown here due to the limited space, other visualizations of 3D vortices and 2D-contours on plane sections reinforced the point that a DES solution yields a much richer description of the flow conditions than the RANS solution. In terms of the unit hydraulic

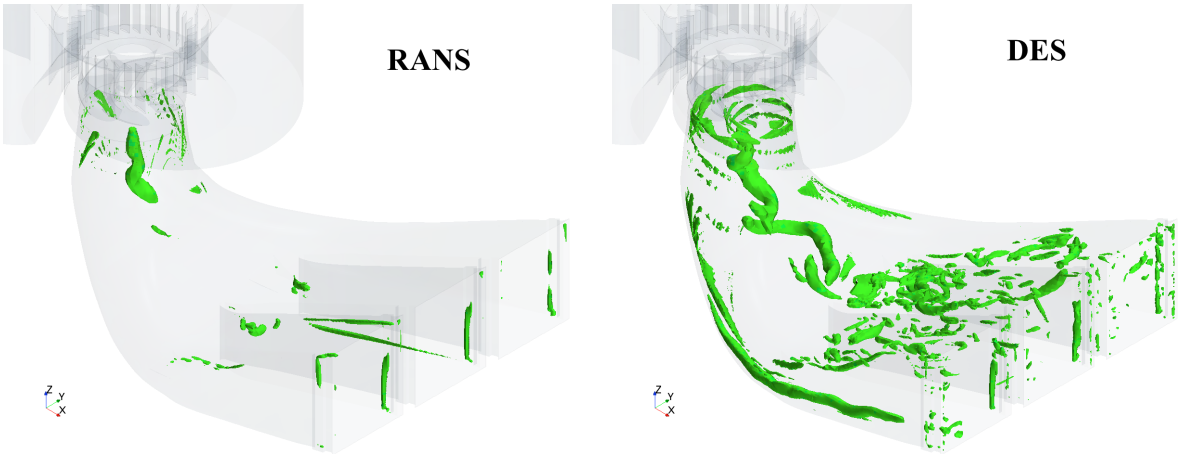

Figure 4. Isosurfaces of Q-criteria in the draft tube show the qualitative differences arising from the RANS and DES schemes for turbulence modeling

Table 1. CFD-simulated and plant estimated values of averaged metrics of hydraulic performance

	Discharge, m^3/s	Power, MW	Net head, m	Efficiency, %
Plant estimate	472.13	99.14	22.95	93.27
RANS	476.77	98.86	23.22	91.25
DES	476.74	98.19	23.22	90.65

performance, Table 4.1 lists the discharge, output shaft power, net head and efficiency from the modeling results and the plant estimates. Here we recall that the modeling strategy in CFD was to prescribe the differential pressure between the upstream and downstream water surfaces (gross head) to drive flow through the system. With respect to plant estimates, the modeling results show an increase of 1% in discharge, an increase of 1% in net head, and a decrease of the unit efficiency by 1.5-2.5%. The power values are essentially the same between the field data and RANS results, and a slight decrease was observed from the DES solution. Given the extent of the domain, the computational resources, and the potential absence of minor geometry features that may impact the hydraulic metrics, we judged both methods to produce results of similar quality from the standpoint of bulk hydraulic performance metrics.

Both RANS and DES produced similar levels of TKE_{total} (in J/kg), with values in the order of 10^{-5} at the release points, 10^{-3} near the stay vanes and wicket gates, 10^{-1} underneath the runner, and greater than 1.0 in the draft tube. In terms of the turbulence intensity, averages from the solution sampling probes were in the order of less than 1%, 5%, 3% and 40%, respectively. The trends of TKE and turbulence intensity indicated that the turbulent conditions increased as the fluid moved downstream. The low turbulence at the intake emerged from representing the trash racks as baffles with uniform porous characteristics that generated a pressure drop but very little turbulence, and from not including the test fish release structure actually in place during the field tests and plant estimates. These simplifications will be revisited as part of the future work because they not only have an impact on the turbulence conditions prevailing at the intake, but also have implications on the dispersive motion of particles that are used to evaluate biological performance, as will be discussed below.

4.2. Blade-strike frequency and nadir pressure

The sensor fish (SF) strike events were categorized into severe (Sv), medium (Md), and slight (Sl) strikes based on an algorithm that accounted for the intensity and time span of the acceleration-deceleration spikes during a collision [6]. The SF device does not record the position and trajectory of the instrument during passage, and the "runner" strikes are estimated by means of post-processing the acceleration and pressure time series retrieved from each device [4]. Therefore, SF strikes could also include strikes on the hub and the discharge ring. Figure 5 shows the results from all the evaluation methods, per pipe-elevation. All modeling methods predicted greater blade-strike frequency from 10-ft pipe releases than from 30-ft pipes; however, only the all-inclusive SF data set (Sv+Md+Sl) showed a similar pattern. The other SF data groups exhibited the opposite trend. Because the modeled results include all collisions, it is more likely that the results from the DEM and spherical particles were more consistent with the all-inclusive SF data group. One major difference between the data sources is that the SF-based probability accounted for single and multiple collision events from the same device, whereas the modeling approaches used a single (the first) registered collision to determine a striking particle. From all the modeling approaches, streamtraces feature the smallest difference between the pipe release groups. However, the streamtraces model the probability of strikes only at the blade leading edge while the DEM particles and spheres record collisions over the entire blade surface, hub, and discharge ring.

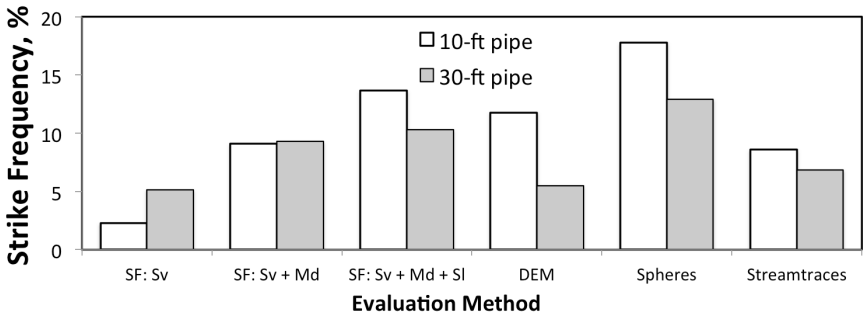

Figure 5. Strike frequency from all the methods, for both release pipe elevations. Sensor fish data classified by Sv = Severe; Md = Medium; Sl = Slight.

Finally, the distributions of nadir pressure recorded from the SF devices and sampled from the three modeling methods are compared in Figure 6 from both pipe-elevation groups. Three observations are noteworthy: first, the simplest modeling technique (streamtraces) showed the best agreement with the SF data; second, DEM particles and spheres display very similar pressure exposures, and third, the three modeling techniques yield, in general, greater values of nadir pressure than SF data. For the first observation, the streamtrace-based method accounted for the circumferential and vertical variability of streamtraces arriving at the stay vanes and wicket gates by applying an algorithm that "spread" the streamtraces to mimic the effect of turbulent dispersion; otherwise, the pipe releases would result in a single passage trajectory through the turbine system. The DEM particles and spheres do account for such turbulent dispersion, but they disperse less than the streamtraces because they are only slightly affected by intake turbulence during the travel from release to the runner, owing to the low TKE and turbulence intensity levels in the intake. This resulted in the second observation, i.e. similar nadir pressure distributions emerged from the DEM particles and spheres. For the third observation, the absolute pressure from all the modeling schemes is currently adjusted by using the average downstream water surface elevation and atmospheric pressure over all the entire period when field tests were performed. In reality, the water surface elevation in the

field may be fluctuating and this should be accounted for in a revised estimate of the absolute pressure as part of the work currently in progress to enhance our understanding of the pressure environment in the system.

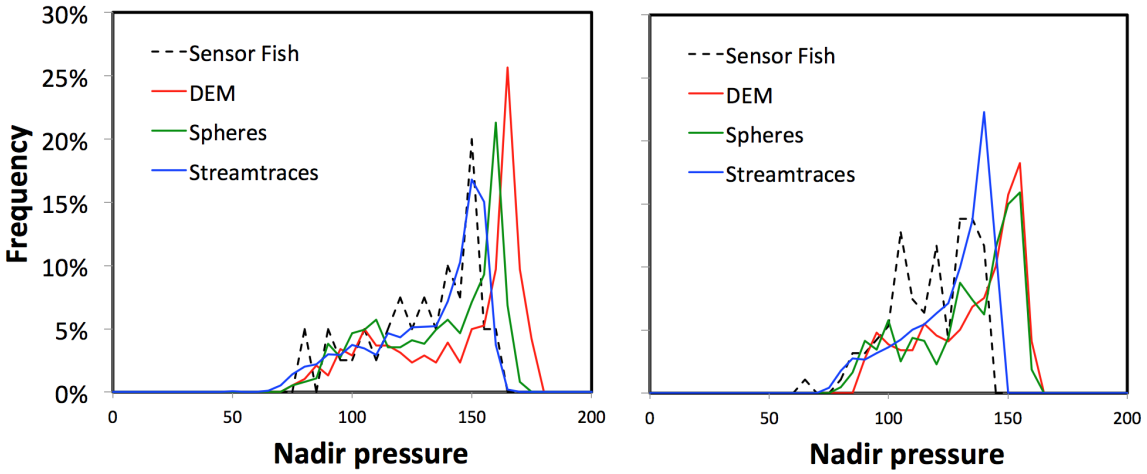

Figure 6. The distribution of nadir pressures from all modeling approaches and SF data, from the "10-ft" (left) and "30-ft" pipe elevations (right)

5. Conclusions and Future Research

This work presented a numerical modeling approach to evaluate the frequency of fish striking moving turbine blades and the distribution of nadir pressures to which a fish may be subjected during turbine passage. The method consists of two main steps: flow description using CFD and fish path estimation using particle tracking. We tested the sensitivity of results to: flow simulation with RANS and DES, and trajectory tracking with streamtraces, Lagrangian, and DEM particles. The streamtrace-based outcomes agreed better with field measurements of nadir pressure than the DEM and spherical particles. This appeared to be mostly due to the turbulent dispersion in the intake accounted for in the former but not in the latter. However, DEM particles offer more advantages to evaluating blade-strike frequency compared to streamtraces because the former account for the mass, full fish length, and width thus resolving (instead of modeling) the collision event.

This research work developed modeling capabilities to estimate biological performance *a priori*, an assessment increasingly necessary for the design of fish-friendly hydropower turbines, and for operation license renewals. We introduced a number of alternatives, compared them to fish data, and recognized their advantages and limitations. Because the refinement of the modeling formulation is still ongoing, the presented findings are not conclusive as to which method is best for representing the hazardous conditions that fish undergo during passage through hydro-turbines. It is quite likely that a range of modeling approaches will be needed for use at different points in the design cycle to balance the desire for greater physical realism against less computational effort to get faster turnaround times.

Our findings point to the need for including additional vorticity producing structural components that will potentially increase the level of intake turbulence, namely the trash racks and test fish release frames. We are currently developing a high resolution model by incorporating these structures into the geometry and by refining the CFD to yield more resolved intake turbulence. In addition, the formulation to model drag force and torque in DEM particles

of irregular shape will be revisited to gain understanding of the fluid forces affecting potential fish pathways, and ultimately, their ability to survive turbine passage.

Acknowledgments
This research was supported by the US Department of Energy, Energy Efficiency and Renewable Energy, Wind and Water Power Program. We thank Brad Strickler and Curtis Dotson of Public Utility District No. 2 of Grant County, Ephrata, Washington for assisting with the project. We also thank Voith Hydro for providing the turbine geometry. Computations described here were performed using the facilities of the Pacific Northwest National Laboratory (PNNL) institutional computing center (PIC). Pacific Northwest National Laboratory (PNNL) is operated for the US Department of Energy by Battelle Memorial Institute under Contract No. DE-AC06-76RLO 1830.

References

[1] Schilt C R 2007 *Applied Animal Behavior Science* **104** 295–325 ISSN 0168-1591
[2] Cramer F and Oligher R 1964 *Transactions of the American Fisheries Society* **93** 243–250
[3] Čada G, Coutant C and Whitney R 1997 Development of Biological Criteria for the Design of Advanced Hydropower Turbines Tech. Rep. DOE/ID-10578 Idaho National Laboratory Idaho Falls, ID
[4] Dauble D, Deng Z, Richmond M, Moursund R, Carlson T, Rakowski C and Duncan J 2007 Biological Assessment of the Advanced Turbine Design at Wanapum Dam, 2005 Tech. Rep. PNNL-16682 Pacific Northwest National Laboratory Richland, WA
[5] Richmond M C, Serkowski J A, Ebner L L, Sick M, Brown R S and Carlson T J 2014 *Fisheries Research* **154** 152 – 164 ISSN 0165-7836
[6] Deng Z, Carlson T J, Dauble D D and Ploskey G R 2011 *Energies* **4** 57–67 ISSN 1996-1073
[7] Hogan T W, Cada G F and Amaral S V 2014 *Fisheries* **39** 164–172
[8] Carlson T, Duncan J, Gilbride T and Keilman G 2004 *Sensors Magazine* **21** 31–34
[9] Deng Z, Carlson T J, Duncan J P and Richmond M C 2007 *Sensors* **7** 3399–3415 ISSN 1424-8220
[10] Normandeau Associates, Skalski J R and Townsend R L 2005 Performance Evaluation of the New Advanced Hydro Turbine (AHTS) at Wanapum Dam, Columbia River, Washington Tech. rep. Normandeau Associates Inc Drumore, Pennsylania
[11] CD-adapco 2013 *User Guide, STAR-CCM+ Version 8.02* (http://www.cd-adapco.com: CD-adapco)
[12] Richmond M C, Rakowski C L, Serkowski J A, Strickler B, Weisbeck M and Dotson C L 2013 *HydroVision 2013* (Pennwell)
[13] Richmond M C, Deng Z, McKinstry C A, Mueller R R, Carlson T J and Dauble D D 2009 *Fisheries Research* **97** 134–139 ISSN 0165-7836
[14] Von Raben K 1957 *Die Wasserwirtschaft* **4** 97–100
[15] Ploskey G and Carlson T 2004 Comparison of blade-strike modeling results with empirical data Tech. Rep. PNNL-14603 Pacific Northwest National Laboratory Richland, WA
[16] Amaral S and Hecker G 2008 Evaluation of the Effects of Turbine Blade Leading Edge Design on Fish Survival Tech. Rep. 1014937 Electric Power Research Institute
[17] Hunt J, Wray A and Moin P 1988 *Proceedings of the Summer Program 1988* CTR-S88 (Center for Turbulence Research) Stanford, CA